STUDY OF PIEZOELECTRIC VIBRATION HARVESTER BASED ON CLAMPED-GUIDED BEAMS UNDER SHOCK EXCITATION

Z. Wang, R. Elfrink, M. Renaud, R. J. M. Vullers, and R. van Schaijk
Holst Centre/imec, High Tech Campus 31, 5656AE, Eindhoven, The Netherlands

Abstract: This paper addresses the output performance of a piezoelectric vibration harvester based on clamped-guided beams under shock excitations. In shock-driven applications, the power output is not restricted by the previously observed nonlinear behavior under sinusoidal excitation. The harvester has been characterized under both square and half-sine shocks generated on a shaker. The experimental results and their implication to automotive application and reliability study are discussed.

Keywords: piezoelectric vibration harvester, shock excitation, clamped-guided beams

INTRODUCTION

The past few years have witnessed substantial interest in piezoelectric vibration harvesters, which are widely regarded as an enabling technology to realize the energy autonomous tire pressure monitoring system (TPMS). A variety of piezoelectric vibration harvesters have been made in different geometries, of different materials and with different fabrication technologies [1-3]. Despite the observed diversities, most miniaturized harvesters are embodied in the shape of a cantilever beam with an attached seismic mass. The oscillation amplitude of a cantilever beam is restricted by the limited space within their packages. This problem becomes more pronounced at lower resonance frequency and larger vibration amplitude, leading to insufficient power output. Moreover, frequent collisions with the packages can cause the fracture of cantilever beams, resulting in a shortened lifetime.

In an effort to address the aforementioned issues, we have previously developed a piezoelectric vibration harvester based on clamped-guided beams [4]. This type of device shows nonlinear behavior in the frequency sweep of sinusoidal excitation [4-6]. This paper focuses on the output performance of the same device, when subject to shock excitations. Shock excitation is relevant to the evaluation of vibration harvesters for automotive applications. Mounted on tires, harvesters are exposed to periodical shocks every time when they hit the road surface [1]. In addition, shock tests are indispensible for the study and improvement of device reliability, as mandated by various industrial standards [7].

DESIGN

As schematically exhibited in Fig. 1, the vibration harvester consists of one seismic mass and two trusses. The seismic mass is connected to the trusses via two mass beams whereas the two trusses are anchored to the silicon substrate via four truss beams. The structural geometry ensures that the seismic mass and the trusses move up and down without tilting, when excited in the "*z*" direction. In this case, the beams can be considered as the clamped-guided type, in which both tensile and compressive stress is developed on all the six beams.

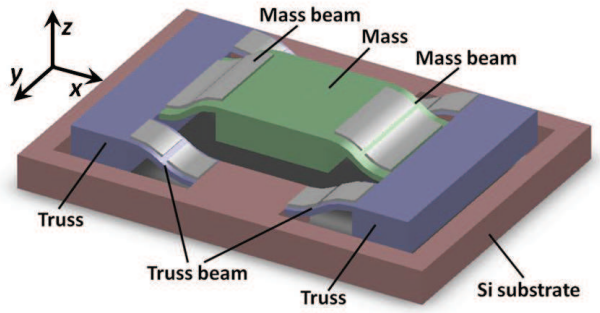

Figure 1: Schematic design of a piezoelectric energy harvester based on clamped-guided beams (not drawn to scale). The trusses are designed with a minimal dimension in the x direction [4].

In view of the presence of both tensile and compressive stresses, two separate capacitors are designed on each beam. These two capacitors on each beam produce a voltage of opposite polarities at the same time. This feature is in contrast to the cantilever-based vibration harvesters, in which the beam supports only one capacitor. As shown in Fig. 2, all the capacitors subject to the same type of stress are connected electrically in series to boost the output. The two sets of capacitors are denoted with "+" and "-". They can be connected in series or in parallel to enhance either the voltage or current output.

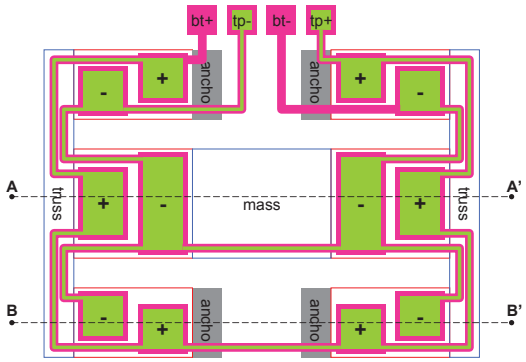

(b)

Figure 2: Each beam has two separate capacitors. Two sets of capacitors, denoted with "+" and "-", are formed via routing [4]. The scheme is not drawn to scale.

FABRICATION

In this work, the vibration harvesters are fabricated with a MEMS processes and packaged in vacuum (Fig. 3). Platinum (Pt), Aluminum Nitride (AlN) and Aluminum (Al) layers are sequentially deposited and patterned to form the capacitors on a 6-inch SOI wafer. The AlN layer is 1.2 μm thick. The mass, the trusses and the beams are formed by deep reactive ion etching (DRIE) process (Fig. 3(a)). The Si beams are 50 μm thick. The glass wafers for encapsulation are etched to form deep cavities and coated with SU-8 layer by using roller-coating method (Fig. 3(b)). The device wafer is then vacuum bonded to the two glass wafers (Fig. 3(c)) and finally diced (Fig. 3(d)).

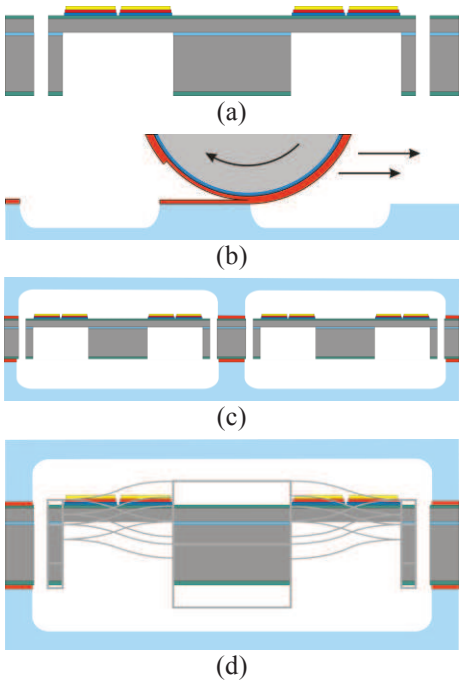

(a)

(b)

(c)

(d)

Figure 3: Cross-sectional schematic fabrication process flow (not drawn to scale). In (d), the vibration mode of interest is also illustrated [4].

EXPERIMENTS

Square shocks

One device with a resonance frequency of 726Hz is measured under square shocks generated by a shaker. The two sets of capacitors are connected in series, giving rise to a total capacitance of 1.8nF and a matched load of 241kΩ. The square shocks are of 20g in magnitude and 0.7msec in duration. The blue-colored curve shows the ring-down behavior of the voltage output over a period of 100msec after the shock. The slow ring-down behavior is attributed to the high quality factor of the device, i.e. ~660.

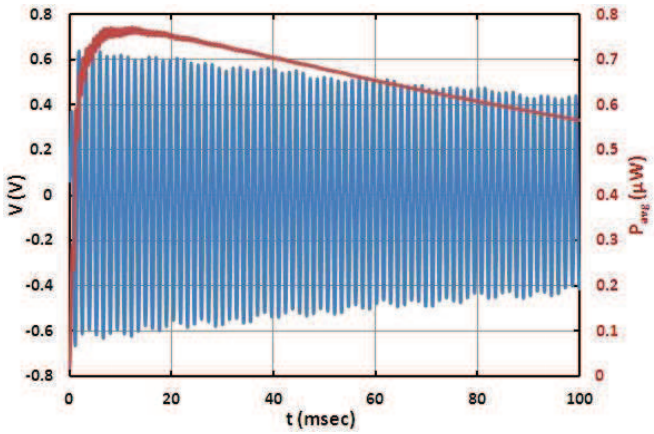

Figure 4: Voltage output and moving average power output on a matched load of 241kΩ after a square shock of 20g and 0.7msec.The two sets of capacitors are connected in series.

As depicted by the red-colored curve in Fig. 4, the moving average power output P_{avg} gradually decreases over time. It is defined as

$$P_{avg} = \frac{\int_0^t \frac{V(t)^2}{R} dt}{t} \qquad \text{Eq. (1)}$$

where $V(t)$ is the instantaneous voltage output, R is the matched load and t is the time variable. For 100msec after the square shock of 20g, the average power output amounts to 0.57μW. A time interval of 100msec between shocks is obtained at the speed of about 70km/h on a tire of type 205/55R16. For the purpose of comparison, the average power output is always calculated for a period of 100msec in this paper.

Alternatively, the two sets of capacitors can be connected in parallel, resulting in a lower matched load, i.e. 60kΩ., The voltage output under the same shock conditions is halved in comparison to the case

of serial connection, as illustrated in Fig. 5. The current through the load is doubled and consequently, the moving average power output remains almost unchanged for the same period after the shock.

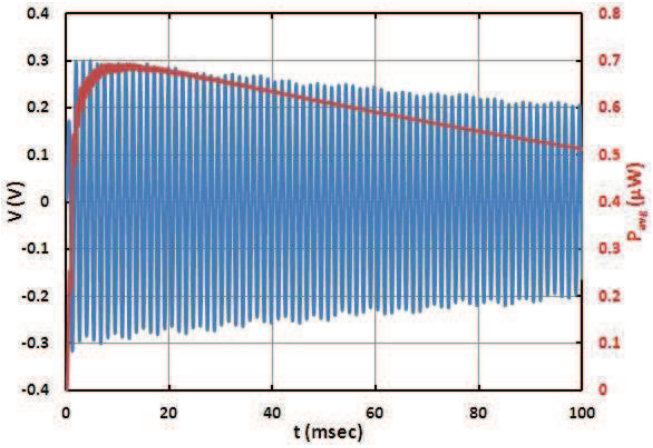

Figure 5: Voltage output and moving average power output on a matched load of 60kΩ after a square shock of 20g and 0.7msec.The two sets of capacitors are connected in parallel.

For square shocks of a fixed duration, e.g. 0.7msec, the average power output is quadratically proportional to the shock magnitude, as indicated in Fig. 6. For a square shock of 90g the average power output after 100msec reaches 11.76μW. This is in contrast to the linear relationship with input acceleration beyond certain value in the frequency sweep of sinusoidal excitation [4]. In other words, the nonlinear behavior that limits the power output is not observed in shock-driven applications. In car tires, the shock magnitude is quadratically proportional to the speed. A shock magnitude of 90g is obtained at the speed of about 60km/h on a tire of type 205/55R16. Thus, an even larger power output is expected beyond 60km/h.

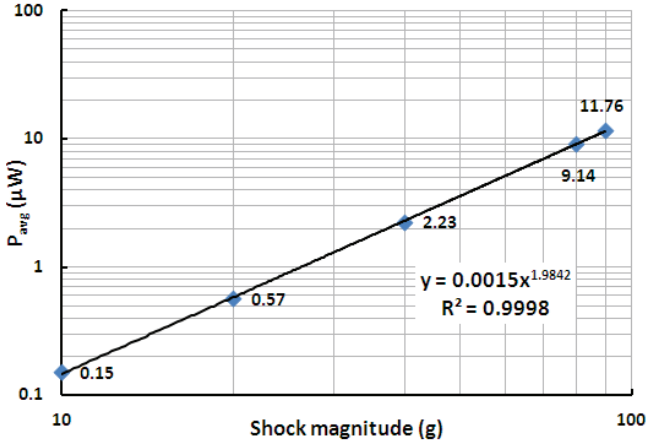

Figure 6: Average power output (for 100msec after the shock) on a matched load of 241kΩ under square shocks of variable magnitude (from 10g to 90g).

The average power output depends not only on the shock magnitude but also on the shock duration t_{shock}. Fig. 7 shows the average power output over a fixed period of 100 msec after the shock for variable shock durations. For square shocks, the maximum power output is generated when the shock duration t_{shock} is odd times as long as half of the harvester period T, namely T/2, 3T/2 and so on [8]. In this case, the shocks are fully constructive to the power generation of harvesters. On the other hand, no power can be produced when the shock duration t_{shock} is even times as long as the harvester period, namely T, 2T and so on. Consequently, the shocks are fully destructive to the power generation. This observation is relevant to the prediction of power output from harvester mounted in car tires, where the shocks can be considered as square shape.

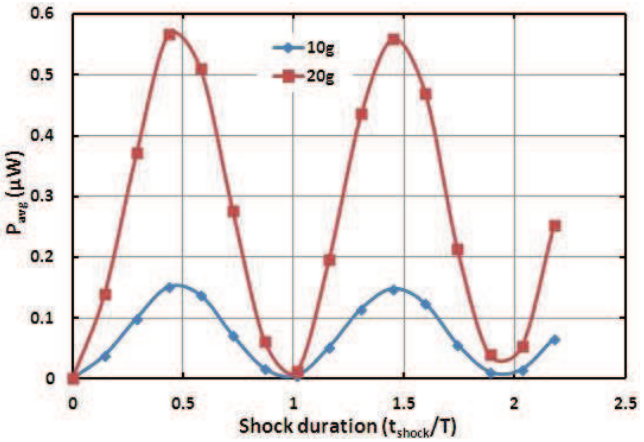

Figure 7: Average power output (for 100msec after the shock) on a matched load of 241kΩ under square shocks of variable duration. The shock duration t_{shock} is normalized to the harvester period T.

Half-sine shocks

A different dependency with the shock duration has been observed for the half-sine shocks. The half-sine shocks are widely used for reliability qualification of devices deployed in automotive applications, as mandated by the relevant industrial standards [7]. Fig. 8 shows the average power output of the same harvester over 100msec for variable shock durations. The maximum power output is obtained when the shock duration is equal to about 0.68T. Despite its periodicity, the maximum power output decreases fast with a longer shock duration. The observed dependence on the shock duration is relevant to the worst case scenario in the drop tests for reliability qualification. Note that the maximum power output is associated with the maximum mass displacement. Therefore, the shock reliability test should be carried out with the duration of 0.68T for the worst case

scenario, in which the maximum mass displacement takes place. Large magnitude half-sine shocks, as from 100 g, can be generated on a drop tester.

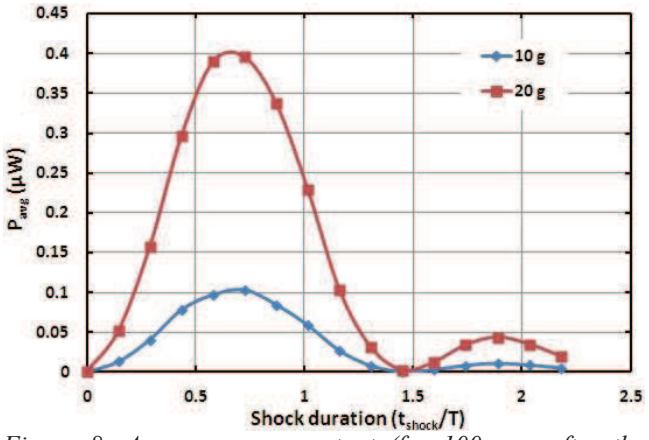

Figure 8: Average power output (for 100msec after the shock) on a matched load of 241kΩ under half-sine shocks of variable duration. The shock duration t_{shock} is normalized to the harvester period T.

DISCUSSION

The two sets of capacitors can be connected either in series or in parallel, leading to different impedances in the two cases. Despite almost the same power output on a matched external load, the voltage output differs by a factor of 2. A higher voltage output is in general desired, because the efficiency of voltage up-conversion can thus be increased.

The measurement results of power output under shock and half-sine shock excitations are relevant to automotive applications and reliability study, respectively. When mounted in tires, a harvester is subject to square shocks of variable duration, which is inversely proportional to the speed. Thus, the actual power output of harvester is highly dependent on the instantaneous speed. In comparison, a different correlation of power output with shock duration is verified for half-sine shocks. This fact means that certain shock duration, i.e. 0.68T, should be used in the drop tests for the worst case scenario.

CONCLUSION

The characterization of piezoelectric vibration harvesters featured by clamped-guided beams is presented in this paper for shock excitation. The analysis is performed in view of automotive applications and device reliability study. Moreover, in shock-driven applications, the previously observed nonlinear behavior can be avoided. After shock excitations, the piezoelectric harvester oscillates only at its natural frequency. The power output is independent of the connection of two sets of capacitors. An average power output of more than 10μW can be produced under a square shock of 0.7msec and 90g. As shown experimentally, the power output depends on the shock duration in different ways for square and half-sine shocks. The implication to the automotive application and reliability study is also discussed.

REFERENCES

[1] Elfrink R., Matova S., de Nooijer C., Jambunathan M., Goedbloed M., van de Molengraft J., Pop V., Vullers R. J. M., Renaud M., van Schaijk R. 2011 Shock Induced Energy Harvesting with a MEMS Harvester for Automotive Applications *Proc. IEDM 2011(Washington DC, USA, 5-7 December 2011)* 29.5.1-29.5.4

[2] Aktakka E. E., Peterson R. L. and Najafi, K. 2011 Thinned-PZT on SOI Process and Design Optimization for Piezoelectric Inertial Energy Harvesting *Proc. Transducers 2011(Beijing, China, 5-9 June 2011)* 1649-1652

[3] Quintero A. V., Briand D., Janphuang P., Ruan J. J., Lockhart R. and de Rooij N. F. 2012 Vibration Energy Harvesters on Plastic Foil by Lamination of PZT Thick Sheets *Proc. IEEE MEMS 2012(Paris, France, 29 January-2 February 2012)* 1289-1292

[4] Wang Z., Matova S., Elfrink R., Jambunathan M., de Nooijer C., van Schaijk R. and Vullers R. J. M. 2012 A Piezoelectric Vibration Harvester Based on Clamped-Guided Beams *Proc. IEEE MEMS 2012(Paris, France, 29 January-2 February 2012)* 1201-1204

[5] Hajati A. and Kim S.-G. 2011 Ultra-wide Bandwidth Piezoelectric Energy Harvesting, *Applied Physics Letters*. **99**, 083105

[6] Marzencki M., Defosseux M. and Basrour S. 2009 MEMS Vibration Energy Harvesting Devices with Passive Resonance Frequency Adaption Capability, *IEEE J. MEMS*, **18**(6), 1444-1453

[7] JEDEC Standard, Mechanical Shock, JESD22-B104-B, Mar. 2011

[8] William T. Thomson and Maria D. Dahleh, Theory of vibration with applications 5th ed. ISBN 0-13-651068-X 1998